High-Speed and Lightweight Humanoid Robot Arm for a Skillful Badminton Robot

Shotaro Mori [iD], Kazutoshi Tanaka [iD], Satoshi Nishikawa [iD], Ryuma Niiyama, and Yasuo Kuniyoshi [iD]

Abstract—Sports, especially badminton, require participants to perform dynamic and skillful motions. Previous robots have had difficulty in performing like a human because of their severe limitations of low operating speed, heavy bodies, and simplistic mechanisms. In this letter, we propose a new robot design that consists of a structure integrated with pneumatic actuators and noninterfering many-degree-of-freedom joints, for the realization of a high-speed and lightweight humanoid robot. We made a four-degree-of-freedom robot arm for badminton, which is an especially dynamic sport, aiming for maximum speed while meeting geometric requirements. The robot swung with a racket-head speed of 21 m/s, which is a value higher than speeds achieved by previous robotic arms. The robot also realized a skillful shot, namely the spin net shot, which cannot be performed by previous badminton robots having simple mechanisms. A pneumatic robot is considered difficult to control, especially in terms of feedback control. We found that the reproducibility of the robot was as fine as 10–40 mm at the racket head for four kinds of strong swings. Using feedforward control, we also conducted an experiment in which the robot hits a flying shuttle, and achieved a high hitting rate of 69.7% for powerful swings. We believe that this research expands the possibilities of the pneumatic robot and is the first step toward developing a skillful humanoid badminton robot.

Index Terms—Hydraulic/pneumatic actuators, mechanism design, tendon/wire mechanism, humanoid robots, motion control.

I. INTRODUCTION

R OBOTS have been developed for various sports, such as soccer [1], table tennis [2], and badminton [3]–[6]. Such robots can entertain people through their play and are a subject of important research themes, such as artificial intelligence, robotics, and machine learning. With technological advances, robots will become useful in events and as practice partners for professional players. However, conventional sports robots are still not comparable to humans, because the emphasis of their
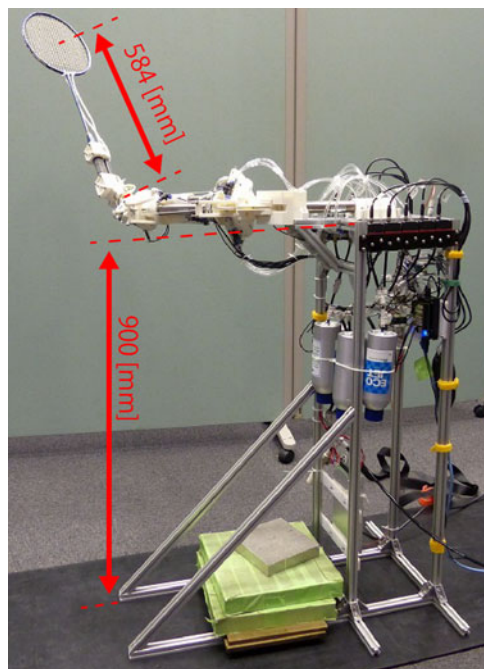
Fig. 1. Overview of the developed robot.

development has mostly been on ensuring the game proceeds even though played clumsily. However, human sports in general require high-speed operation and dexterous action, such as that when hitting a ball in a certain direction in a ball sport, making a fast and skillful attack or avoiding an attack in a fighting sport, or executing a feint.

The present study focuses on badminton as an especially challenging sport for robots demanding dynamic and skillful motions. Badminton is known to be a high-speed game. For example, the initial velocity of the smash is the highest velocity among all ball sports [7]. In addition, badminton has skillful shots that use unique characteristics, such as the lightweight body and complex shape, of the shuttle [8], [9]. Badminton robots have already been developed; e.g., wheeled robots that have participated in a university competition [3], [5], [6] and a railed robot [4]. These robots realized continuous rallies but had only a simple mechanism with few degrees of freedom (DoFs), and they therefore could not perform the varied and skillful shots that humans use. Such shots are effective in terms of deceiving opponents, often determine who wins a match, and excite spectators.

A humanoid sports robot has advantages in that the opponent's motion is important in interpersonal sports; e.g., execut-

ing feints and predicting the opponents next move are important aspects of sport. The high number of DoFs of the humanoid is also effective for the execution of skillful shots as mentioned above.

We therefore consider three requirements of next-generation badminton robots: high speed, low weight, and a humanoid form. Naturally, these requirements relate also to other sports. However, there are many difficulties in realizing all these requirements.

High-speed manipulation is an important theme for general robotic arms. Kawamura *et al.* developed FALCON [10], which realized acceleration of 43 [G] at the end effector (320 [g]) via a parallel-link-wire driving mechanism. However, the maximum speed was no more than 13 [m/s]. Its size is about 1.45 [m] × 1.45 [m] × 1.25 [m]. As a humanoid robot arm, WAM Arm is a well-known high-speed serial-link-type robot, having actuators at the base of a link and employing a wire driving system. Senoo *et al.* realized high-speed batting using WAM Arm [11] with a reach of 1000 [mm], but the maximum speed was no more than 6 [m/s] (and is officially limited to 3 [m/s]). Büchler *et al.* developed Lightweight Robotic Arm [12]. They placed all pneumatic artificial muscles on the base and made the arm itself lightweight (700 [g]), and realized a speed of 12 [m/s] at the end effector for pneumatic pressure of 0.3 [MPa] and angular velocity of 1500 [deg/s] (26.18 [rad/s]). Fast robotic arms have thus been developed using light arms. However, the overall bodies are heavy because the robots have been developed to be stationary; e.g., WAM Arm has a mass of 27 [kg] [13]. Future sports robots should be able not only to swing quickly but also to make fast whole-body movements. In addition, developed robots do not have anthropomorphic joints such as a high-DoF wrist.

Against the above background, as a high-speed and lightweight humanoid robot that can play badminton, we propose a humanoid robot that is actuated by a wire-driven pneumatic cylinder integrated in the structure. As an example, we make a robot with four DoFs from the elbow to hand. We then evaluate the robot and test its ability to return a badminton shuttle.

II. PROPOSED HIGH-SPEED AND LIGHTWEIGHT HUMANOID ROBOT SYSTEM

A. Requirements of the Robot

According to the above discussion, the requirements of a humanoid badminton robot are summarized as the high-speed swing of a human, the anatomical shape of a human, and agile whole-body motion. However, as a minimum setup in the first step of development of such a robot, we made and evaluated a simple four-DoF robot arm. The robot arm comprises only the arm below of the elbow but includes important components for future extension: a three-DoF joint and linking. We focused on the high-speed wrist, which is the fastest-moving joint in the human body and said to be important in a badminton smash [14]. The requirements of the robot arm are then described as follows.

- High-speed wrist as for humans (26.3 [rad/s] [14]);
- The anatomical shape of a human, having DoFs, link lengths, and link diameters similar to those of a human;

①: medial rotation/external rotation
②: pronation/supination
③: palmar flexion/dorsal flexion
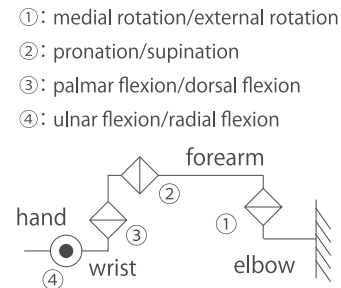④: ulnar flexion/radial flexion

Fig. 2.   DoF diagram of the developed robot.

- Low overall weight and volume for extensibility to an agile whole-body robot.

B. Overview of the Robot

The selection of actuators is most important in realizing such a robot. We employed pneumatic actuators. Among other commonly used actuators, an electromagnetic actuator has a quick response and high controllability. However, its speed is strictly limited by its back electromotive force and its power-to-weight ratio is low because of its heavy coil and magnet. A hydraulic actuator has a high power-to-weight ratio for an industrial machine, but it needs other heavy apparatus such as pumps and motors. Moreover, its speed is limited because of high oil viscosity. Meanwhile, a pneumatic actuator has a much higher power-to-weight ratio than other actuators on the whole, and can realize high-speed motion. One disadvantage of the pneumatic actuator is the requirement of an air compressor. However, there are lightweight compressors available, such as MAX-JET manufactured by NIKKEN (5 [kg], 31 [L/min] at 0.8 [MPa]). Otherwise, it is also possible for the sports robot to be equipped with tanks and for compressed air to be supplied from outside the court through a thin tube. Additionally, a slow response can be a serious problem for the feedback control, but we will propose a feedforward control method that is suitable for the high-speed motion of a pneumatic robot.

The robot (Fig. 1) has a one-DoF elbow and a three-DoF wrist. The robot reproduces the anatomical shape and DoFs of a human. In this letter, we refer to the DoFs of medial rotation/external rotation (elbow joint), pronation/supination (wrist PS joint), palmar flexion/dorsal flexion (wrist PD joint), and ulnar flexion/radial flexion (wrist UR joint). These are shown in Fig. 2. The ranges of joint angles are approximately simulated as those of a human; the UR joint is at 90 [deg] while the other joints are at 180 [deg]. The masses of different parts, including proportional-pressure-regulating valves (Tecno basic, Hoerbiger Corp.) and air tanks (550 [ml]), are low as shown in Table I. The air compressor is placed outside and continuously supplies air to the robot through a tube. Each joint is equipped with a potentiometer to measure the joint angle. The workspace of the robot is shown in Fig. 4.

C. Mechanical Design

The lightweight links of arms are essential for a high-speed swing. Inspired by the Structure Integrated Pneumatic Cable
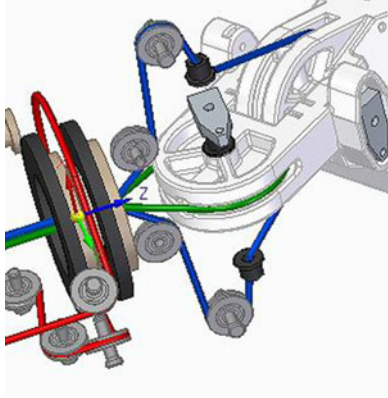
Fig. 3. Wiring diagram of the three-DoF wrist.

TABLE I
MASS AND LENGTH OF EACH PART OF THE ROBOT

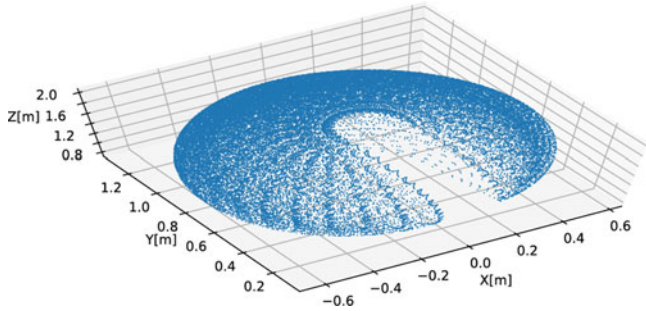| Section	Mass	Note
Upper arm	453 [g]	link#0, Fixed on the base
Forearm	1063 [g]	link#1, 363 [mm]
Hand 1	187 [g]	link#2, 63 [mm]
Hand 2	54 [g]	link#3, 44 [mm]
Hand 3	254 [g]	link#4, 584 [mm], incl. a racket(96 [g])
Air valve	144 [g] × 9	Fixed on the base
Air tank	113 [g] × 4	Fixed on the base, 550 [ml]

Fig. 4. Workspace of the robot. The workspace is approximated as a thin elliptical surface, although part of the space behind the robot is not covered. The lengths of the major axes are approximately x = 1342 [mm], y = 1242 [mm], and z = 1116 [mm].
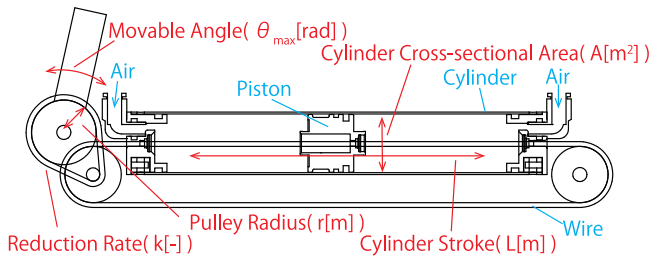

Fig. 5. Simplified robot having an SIPC cylinder and five important design parameters.

(SIPC) cylinder [15], we integrated pneumatic cylinders into links as shown in Fig. 5. Because actuators are integrated in the structure and employ cables instead of the heavy rods used in normal air cylinders, the robot has a lightweight arm and operates with high acceleration and high speed. However, it is difficult to construct an anthropomorphic high-DoF robot simply
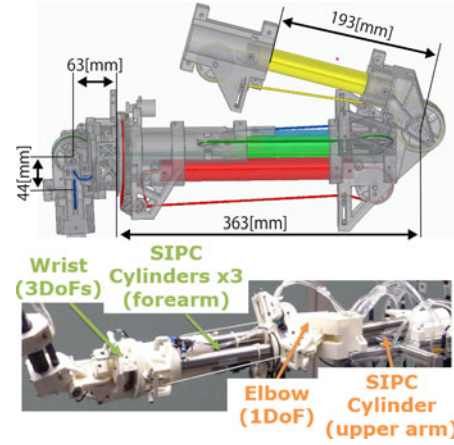

Fig. 6. Configuration of the robot arm.

using a conventional SIPC cylinder as in Fig. 5. We will propose a method of configuring an anthropomorphic robot by placing a plurality of SIPC cylinders on one link and construct multi-DoF joints (Fig. 6). As a precaution when designing multi-DoF joints, it is necessary to devise wire routes so that the wires do not slacken for each posture. We routed wires through relay points on each joint axis to avoid such slackening, and successfully realized a three-DoF wrist (Fig. 3). A link length and diameter similar to those of humans were realized by this design. An entire arm with a shoulder, or a whole-body robot having legs, can be constructed by connecting a plurality of the structures.

D. Determination of Design Parameters

There are trade-off relationships of, for example, the weight, obtained velocity, and specifications of the servo valve. Here, the angular velocity at each joint is especially important, but the angular velocity cannot be simply calculated for a pneumatic actuator. We will show how to calculate the angular velocity at each joint through modeling and simulation and determine design parameters.

There are five important design parameters as shown in Fig. 5, namely the cross-sectional area of the inner cylinder $A[\text{m}^2]$, the pulley radius of the joint $r[\text{m}]$, the cylinder stroke $L[\text{m}]$, the maximum angle of motion $\theta_{\max}[\text{rad}]$, and the reduction ratio $k[-]$. The reducer is not implemented here but can be helpful in adjusting parameters to satisfy geometric constraints, such as an anthropomorphic arm length.

First, $kr\dot{\theta}(t) = \dot{x}(t)$ and $kr\theta_{\max} = L$ should be satisfied, where $\theta(t)$ [rad] is a joint angle and $x(t)$ [m] is a piston position. According to the equation of motion, $\theta(t)$, $x(t)$, and the force produced by the actuator $f(t)$ [N] are

$$I\ddot{\theta}(t) = \mu k r F(t) - \tau_c \text{sgn}\big(\dot{\theta}(t)\big), \tag{1}$$

$$m\ddot{x}(t) = f(t) - F(t) - \big(f_p \text{sgn}\,(\dot{x}(t)) + f_{pv}\dot{x}(t)\big), \tag{2}$$

$$f(t) = (P_+(t) - P_-(t))\,A. \tag{3}$$

For our robot, $(P_+(t) - P_-(t))A \gg f_p \text{sgn}(\dot{x}(t)) + f_v \dot{x}(t)$ and $I \gg \mu m k^2 r^2$ are satisfied when a robot swings under full power.

Then, approximately speaking,

$$\ddot{\theta}(t) \approx \frac{\mu k r A \{P_+(t) - P_-(t)\} - \tau_c \mathrm{sgn}(\dot{\theta}(t))}{I} \quad (4)$$

is satisfied from (1)–(3), where P_+[Pa] and P_-[Pa] denote the pressure of each chamber in a cylinder, τ_c[N·m] is the static friction torque, f_p[N] is the static friction in a piston, f_{pv}[N·s/m] is the coefficient of viscous friction in the piston, m[kg] is the mass of the piston, and I[kg·m/s] is the moment of inertia around the joint. Equation (4) suggests that the robot can increase speed if k, r, and A are set large. However, when a robot operates at high speed, the air pressure decreases owing to an insufficient air flow rate and the obtained speed decreases. This can be considered by modeling the air. By differentiating the state equation of gas, we obtain

$$\dot{P} = \frac{\rho Q R T - k r A \dot{\theta}(t) P}{k r A \dot{\theta}(t) + V_0}, \quad (5)$$

where P[Pa] is the pressure in a chamber, ρ[kg/m^3] is the density of air, R[J/kg·K] is the gas constant, T[K] is the temperature of the gas, and V_0[m^3] is the initial volume of the chamber. The air flow rate Q[m^3/s] is described as

$$Q = \begin{cases} \frac{S P_{up}}{\rho} \sqrt{\frac{2\kappa}{\kappa - 1} \frac{1}{RT} \left\{ \left(\frac{P_{low}}{P_{up}}\right)^{\frac{2}{\kappa}} - \left(\frac{P_{low}}{P_{up}}\right)^{\frac{\kappa+1}{\kappa}} \right\}} \\ \qquad \left(\left(\frac{2}{\kappa+1}\right)^{\frac{\kappa}{\kappa-1}} < \frac{P_{low}}{P_{up}} < 1 \right) \\ \frac{S P_{up}}{\rho} \sqrt{\frac{\kappa}{RT} \left(\frac{2}{\kappa+1}\right)^{\frac{\kappa+1}{\kappa-1}}} \\ \qquad \left(\frac{P_{low}}{P_{up}} \leq \left(\frac{2}{\kappa+1}\right)^{\frac{\kappa}{\kappa-1}} \right) \end{cases}, \quad (6)$$

where κ[−] is the heat capacity ratio of the air and S[m^2] is the effective sectional area in the flow channel [16]. By reference to the commanded pressure P_d[Pa] and pressure in the chamber P, we define an upstream pressure P_{up}[Pa] and a downstream pressure P_{low}[Pa] as

$$P_{up} = \begin{cases} P_s & (P \leq P_d) \\ P & (P > P_d) \end{cases}, P_{low} = \begin{cases} P & (P \leq P_d) \\ P_A & (P > P_d) \end{cases}, \quad (7)$$

where P_s[Pa] is the pressure of a source of air and P_A[Pa] is the atmospheric pressure. S[m^2] is controlled by a valve. We conducted an experiment to estimate the control law:

$$S = \begin{cases} S_{max} & (P_{th} \leq P_d - P) \\ S_{max} \frac{P_d - P}{P_{th}} & (0 \leq P_d - P < P_{th}) \\ -S_{maxout} \frac{P - P_d}{P_{th}} & (-P_{th} \leq P_d - P < 0) \\ -S_{maxout} & (P_d - P < 0) \end{cases}, \quad (8)$$

which means S is basically a constant value S_{max}[m^2], and when the error in P and P_d becomes less than a threshold P_{th}[Pa], the valve employs proportional control such that P converges to P_d.

The numerical calculation of (1)–(3) and (5)–(8) employing the Runge–Kutta fourth-order method allows simulation of the swing speed of each joint. In the approximate equation of motion
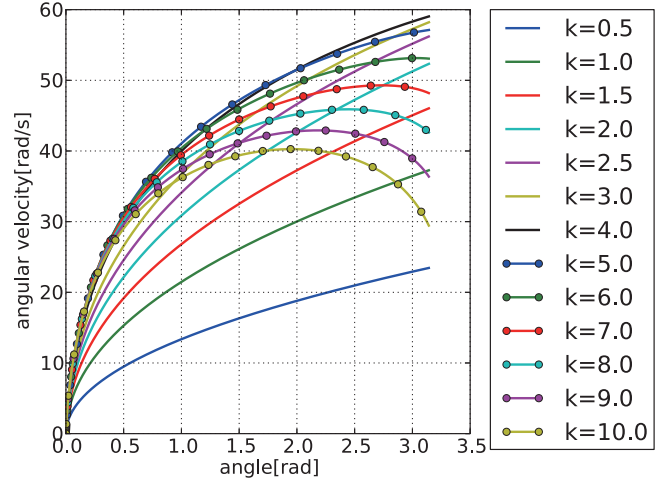

Fig. 7. Relationship of joint angles and angular velocities in swing simulations for different values of the reduction rate parameter (k).

(4) and (5)–(8), all five design parameters emerge as krA. It is therefore enough to adjust only krA in designing the swing speed. An example of the simulation results is shown in Fig. 7 when changing only k in krA and swinging by commanding a step input of 0.7 [MPa]. It is found that when krA is excessive, the speed decreases and the size and weight naturally increase.

A valve specification is also important for the maximum velocity, corresponding to the maximum flow rate S_{max}. A higher value of S_{max} results in a higher maximum velocity at large krA. A valve specification is difficult to design freely, and it would thus be better to first fix a valve and determine krA. Another valve needs to be considered if the speed is excessive or insufficient.

We designed the parameters of wrist PS and PD joints according to the results of simulation; these joints are important to the high-speed swinging of the robot. We decided the parameters such that the joint angular velocity was 40 [rad/s] for the wrist PS joint and 30 [rad/s] for the wrist PD joint at a joint angle of $\pi/2$ [rad] (where the limit of motion is defined as 0 rad). The joint angle was based on the posture at the moment of impact of the smash of the shuttle by a human player, and the velocity was set such that the angular velocity of the wrist joint was 26.3 [rad/s] [14].

III. EVALUATION EXPERIMENTS

A. Evaluation of the Swing Speed

We conducted experiments to confirm the speed generated by the developed robot. We first commanded 0.7 [MPa] at each joint and measured the angular velocity. Results are given in Table II. The speeds of the wrist PD and elbow joints well matched calculated values, but those of the wrist PS and UR joint did not. We believe that friction within a joint having a dry bearing is greater than expected. Nevertheless, the angular velocities of the wrist PS and PD joints, which contribute most to the badminton smash, exceed those of a human, being 26.3 [rad/s] [14]. We next similarly commanded 0.7 [MPa] at the elbow joint and the wrist PS joint with appropriate timing, and attempted to make the robot swing as quickly as possible. A motion capture

TABLE II
SWING SPEEDS OF EACH JOINT FOR A STEP PRESSURE COMMAND (0.7 [MPA])
WHEN THE JOINT ANGLE IS $\pi/2$ [rad] (WHERE CIRCLED NUMBERS ARE
EXPLAINED BY REFERENCE TO FIG. 2)

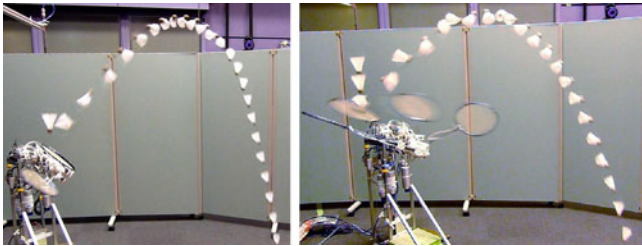| Joint	Angular velocity [rad/s]
Medial rotation (①, elbow joint)	15.7
Ulnar flexion (②, wrist UR joint)	24.2
Palmar flexion (③, wrist PD joint)	29.0
Pronation (④, wrist PS joint)	32.4

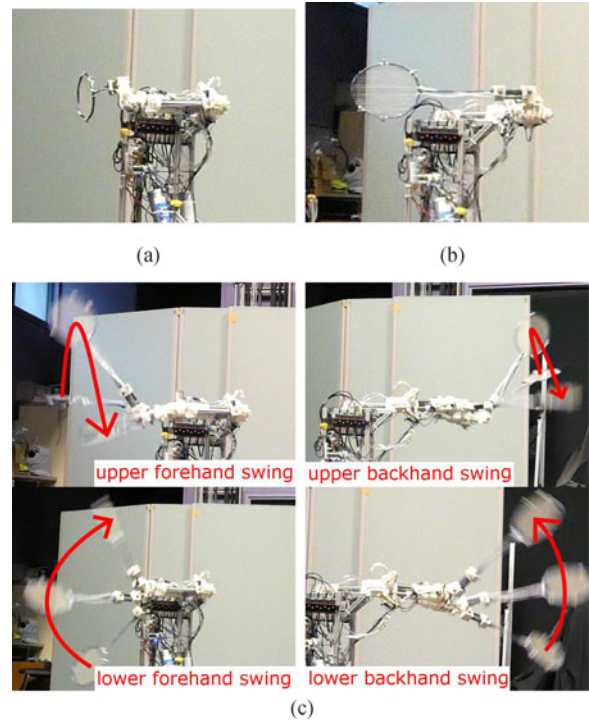Fig. 8. Sequential photographs of a normal net shot (left) and a spin net shot (right).

Fig. 9. Four types of swing used in the reproducibility evaluation and hitting experiment. (a) Initial posture in the reproducibility experiment. (b) Initial posture in the hitting experiment. (c) Four types of swing.

system (VICON624) was used for the measurement. When the joint angle of the PS joint was approximately 90 [deg], the velocity of the center of the racket head was about 21 [m/s]. This is much higher than velocities for previously developed fast robotic arms with the same scale described in Section I, such as WAM Arm [13] (8 [m/s] [11]), Lightweight Robotic Arm [12] (12 [m/s], 26.18 [rad/s]), and FALCON [10] (13 [m/s]).

B. Example of a Skillful Shot—Spin Net Shot

Humans can execute skillful shots using a multi-DoF arm, while a robot can also make such shots when designed as a humanoid. As an example, we had the robot execute a spin net shot. This shot is a slicing motion of the racket surface across the shuttle performed near the net. The shot makes the shuttle spin and tumble, which in turn makes it difficult for the opponent to return the shuttle, especially from a high position. The execution of the shot is a difficult skill even for an expert player, but the shot is often effective and even a winning shot. For the robot to make the shot, we first made the robot adopt an initial posture through proportional-integral-differential (PID) position control. A shuttle was then dropped from above by a vacuum holder, and the robot executed a command prepared in advance. The wrist UR joint was mainly used for slicing, but the wrist PD joint was also needed to return the shuttle forward. Video imagery showed that the shuttle was spinning and tumbling, and it took longer for its cork to face down than in the case of the normal net shot. The robot therefore succeeded in executing the spin net shot (Fig. 8).

C. Reproducibility

In general, feedback position control is employed for robotics control, but such control is difficult for pneumatic robots owing to the slow response or high friction. Pneumatic robots are therefore often said to have poor controllability. However,

feedforward control by learning or preliminary simulation can be a good alternative. To realize feedforward control by a robot, it is necessary to reproduce the motion using the same input. We evaluated reproducibility by executing a certain feedforward command and measured the variance.

The initial posture corresponded to the maximum joint angle and four types of swing were performed by manual programming (Fig. 9). Each swing was strong; the maximum pressure command was 0.65 [MPa], the swing was complete in about 0.10 [s], and the maximum speed of the racket head during the swing was about 11 [m/s] for lower swings and 17 [m/s] for upper swings. We also had the robot first perform a preparatory motion (i.e., a backswing); the total swing time was about 0.70 [s]. Commands were given to all joints so that no joint was at its maximum joint angle during the swing. Calculated standard deviations are presented in Fig. 10.

It was found that, despite the high swing speeds, standard deviations of the racket position were only about 10–40 [mm]. These values are smaller than the racket diameter of about 220 [mm], and we can therefore say that feedforward control is available. The standard deviation of the forehand upper swing was larger than the standard deviations of other swings. Although we do not clearly explain this, the result suggests that some motions are relatively sensitive and the reproducibility differs depending on the command.

IV. HITTING EXPERIMENT

We argued in Section III-C that feedforward control is available for our robot with low controllability. We will show the
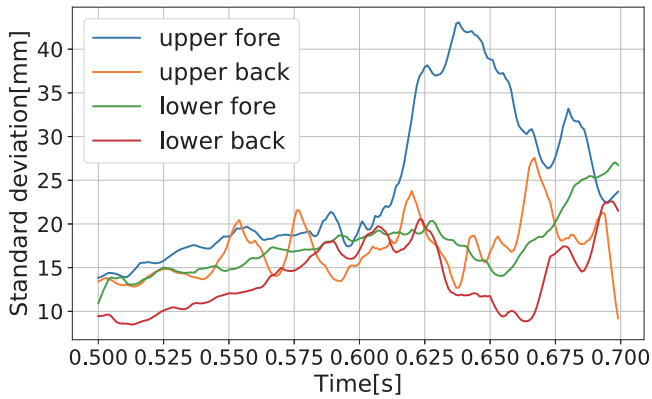
Fig. 10. Time series of the standard deviation of the center position of the racket head for four types of swing in evaluating reproducibility. The timing of the backswing command was 0.00–0.50 [s] while that of the swinging command was 0.50–0.70 [s]; only the swinging time is shown. The position was calculated from each joint angle obtained by the potentiometers approximately every 0.008 [s] and linearly interpolated. There were 12 trials per type of swing.

effectiveness of the control method in a practical experiment of the hitting of an incoming shuttle. Naturally, it is essential for the badminton robot to return a shuttle and so the experiment also shows the extent to which our robot can play a real game of badminton.

A. Shuttle Trajectory Recognition and Prediction

We used a motion capture system (Prime 13 W x8, Opti Track, 240 fps) to recognize a flying shuttle. Reflective tape was put on the cork of the shuttle but had little effect on the flight characteristics because the tape was thin and light. Following previous studies [4], [5], the shuttle position and velocity were estimated from a measurement time series and the trajectory was predicted using an aerodynamics model.

B. Motion Training and Selection

We tried the most basic method of feedforward control to generate hitting motions in the present study. We had the robot perform various swings via feedforward pressure commands, and memorize the motions and corresponding commands preliminarily. When a shuttle was incoming, the robot selected an appropriate command for hitting the shuttle. The motion selection algorithm is presented as Algorithm 1, and the overall hitting algorithm as Algorithm 2.

We first generated four patterns of swings by manual programming similar to that in the reproducibility experiment (Section III-C, as shown in Fig. 9). For each swing, we first had the robot take the same initial posture as in the reproducibility experiment according to the motion limit (Fig. 9(a)). However, to start the swings as early as possible, the robot then adopted an intermediate initial posture by executing a certain command for the elbow joint (Fig. 9(b)). We confirmed the robot could well reproduce the initial posture. We generated 37 patterns of swings by slightly changing the commands. For each swing, an appropriate time range for hitting was extracted, and the positions of the center of the racket head and the time stamps were recorded (Fig. 11). To return the shuttle forward and

---

Algorithm 1: Command Selecting Algorithm.

Load pretrained swings
//Each swing has measurement points
//Each point has position $\mathbf{P}_{\mathbf{racket}}$ and time t
function Select Swingt_{now}
    Errors=$\emptyset$
    for Each memorized swing **do**
        for Each memorized point **do**
            $\mathbf{P}_{\mathbf{racket}} \Leftarrow$ the racket position at the point
            $t \Leftarrow t_{\mathrm{now}}$ + the time at the point
            for Δt in $[0.0, \Delta t_{\max}]$ **do**
                //Adjusting swing timing
                Errors $\Leftarrow ||\mathbf{P}_{\mathbf{shuttle}}(t + \Delta t) - \mathbf{P}_{\mathbf{racket}}||$
    if $\Delta t = 0.0$ at argmin(Errors) **then**
        return Command at argmin(Errors), min(Errors)
    else
        return Command = None, Error = ∞

Algorithm 2: Overall Hitting Algorithm.

loop
    Taking the initial posture
    repeat
        $t_{\mathrm{now}} \Leftarrow$ current time
        $\mathbf{C}_{\mathbf{exe}}$, Error $\Leftarrow$ SELECT SWINGt_{now}
        if Error $< \mathrm{E}_{th}$ **then**
            Execute the command $\mathbf{C}_{\mathbf{exe}}$
    until Command is executed
    $t_0 \Leftarrow$ current time $\triangleright$ Swing start time
    Repeat $\triangleright$ Command change loop
        $\mathbf{C}_{\mathbf{new}} \Leftarrow$ SELECT SWING$t_0, \Delta t_{\max} = 0.0$
        $t_1 \Leftarrow$ current time
        if $(\mathbf{C}_{\mathbf{exe}} = \mathbf{C}_{\mathbf{new}})$ in $[t_0, t_1]$ **then**
            Change the command to $\mathbf{C}_{\mathbf{new}}$
            $\mathbf{C}_{\mathbf{exe}} \Leftarrow \mathbf{C}_{\mathbf{new}}$
    until The swing finishes

---

dynamically, we chose the time range in which the velocity of the racket head was in the forward direction and the speed was near its maximum, which is effective in making a good shot.

The executing command was chosen so that the racket head and shuttle had the closest approach. In other words, when a shuttle was incoming, the position of the shuttle at the time for each recorded racket head point was predicted, and distance errors were calculated. The swing was executed if the minimum error was less than a certain threshold. The threshold was set to 100 [mm] with reference to the radius of the racket head. If there was no appropriate swing, the algorithm proceeded to the next loop and repeated the same calculation for the new shuttle position. Additional processes were implemented for better performance; the execution of the command was delayed if the error was expected to be smaller ("Adjusting swing timing" in Algorithm 1), or the command was changed after the start of the swing if there was a better command ("Command change loop" in Algorithm 2). The trajectory prediction and selecting
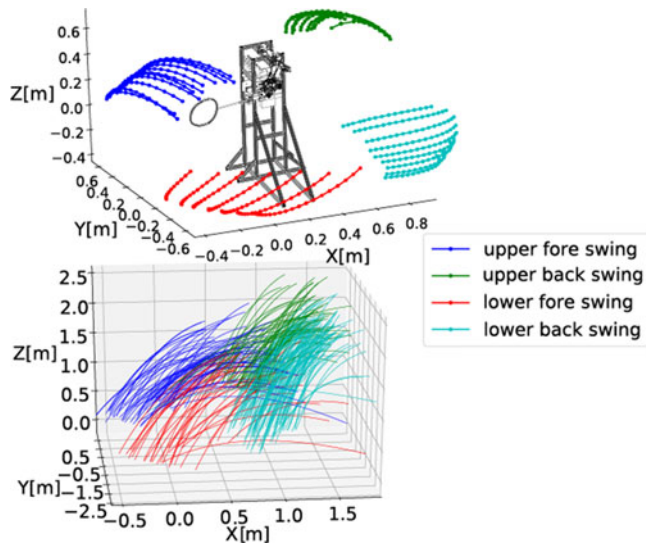
Fig. 11. Trajectories of racket heads in trained swings and trajectories of shuttles served by humans in the hitting experiment. The shuttle trajectories are shown only when the robot swings.

TABLE III
RESULTS OF THE HITTING EXPERIMENT (WHERE DATA WERE RECORDED ONLY WHEN THE ROBOT EXECUTED A SWING)

Swing type	Hit	Just touching	No hit	Total
Upper forehand	46	11	12	69
Upper backhand	17	5	9	31
Lower forehand	39	7	4	50
Lower backhand	65	19	6	90
Total	167(69.7%)	42(17.5%)	31(12.9%)	240

command were processed by an external computer, and the command was then sent to the microcomputer mounted on the robot by socket communication.

C. Results and Analysis

For the above setup, a human served a shuttle from the same position, about 5 [m] away, toward the robot and the robot attempted to return the shuttle. Statistical results are presented in Table III. Although results depended on the type of swing, the hitting success rate was 69.7% over all trials and complete misses accounted for only 12.9% of trials. Sequential photographs of a strike are shown in Fig. 12. The serves made by the human varied (Fig. 11), but the result was recorded only when the robot decide to swing. The results of trials with a large shuttle position error due to the human were therefore removed. The human-serving setup of the experiment also shows that the robot can cope with a certain variety of shots.

Analysis of the results revealed three major reasons why it was not certain that the robot hit the shuttle: shuttle trajectory prediction error, measurement and command delay, and mechanical degradation.

In terms of the first reason, differences between the predicted shuttle positions and the actual shuttle positions can affect the

results. The analysis showed that the prediction before about 0.4–0.5 [s] was used, and the average error was 37 [mm] (0.4 [s] before)–45 [mm] (0.5 [s] before). A shuttle was served with a slow and arched trajectory as shown in Figs. 11 and 12, but the shuttle was more than 2 [m] ahead of the robot at that time. We employed the flying shuttle model that has been commonly used in previous studies [5], [6], but it is a simple model that does not completely express flight characteristics. For example, it has been reported that the spinning and posture of a shuttle may affect the flight characteristics of the shuttle [8], [9], but the effect is not considered in the present model. We have to improve also the shuttle prediction method in designing a more sophisticated robot system.

In terms of the second reason, analysis of the observation results of motion capture showed a slight timing shift even for the same command. Because the sensor data of the robot were not delayed, the timing shift was due to the delay in communication between the motion capture and the external computer or the external computer and the robot. The delay was 0.015 [s] at most from the measurement, but because the swings were fast, even a delay of several milliseconds introduced error. We do not deal with this problem here, but will address it by constructing a system with a shorter communication delay or a system that can be well synchronized.

In terms of the third reason, deteriorations can affect the motion although the reproducibility over a short period is good. Despite training twice again in the middle of the experiment, the motion gradually changed. We estimate the most critical deterioration would be a friction change of dry bearings in joints and wire relay points, which are readily worn away. The effect will be reduced if the dry bearings are replaced with roller bearings, but there could be other deteriorations such as a friction change of a piston, a stretching wire, or response change of a valve. The swings are so strong that deterioration of the robot cannot be completely avoided in long-term operation. The problem can be solved by designing a system where not only is the robot trained in advance but also training results are collected on line.

In this experiment, the effectiveness of the feedforward control method used by our proposed robot is demonstrated to some extent. We admit the method is basic and not robust enough in its present form, but it can be extended in the future. The robot will also become able to return the shuttle with planned direction and power by considering not only the position of the racket head but also the velocity or face directions in the command selecting algorithm. However, this requires more training data. Such commands can be automatically generated with less training by employing simulations or a machine learning approach. For example, the movement changes can be predicted when changing the command without training by the robot model. It is difficult to model a pneumatic robot completely, but learning the robot dynamics model can be helpful [17]. Rather than having a complete dynamics model, the dynamics of similar swings can be easily learned. The deterioration problem can also be solved if the trained trajectories are adjusted by the learned model on line.
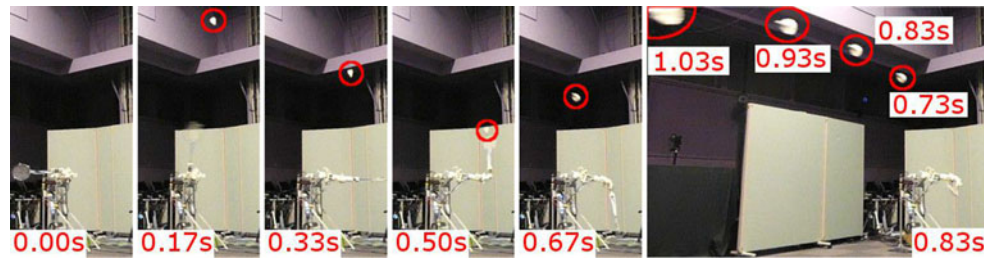
Fig. 12.   Sequential photographs of hitting an incoming shuttle (using a upper backhand swing).

V. Conclusion

We proposed the concept of a high-speed and lightweight humanoid robot system using an SIPC cylinder for an agile sports robot especially designed for badminton, and made a forearm robot as a minimum setup. We successfully implemented a non-interference driven three-DoF wrist by arranging a plurality of SIPC cylinders on one link and devising ways of tying the wires while maintaining low weight. Evaluation experiments showed that the developed robot generates a much higher head speed during a swing than all previous fast robotic arms as far as we know. Despite this, the developed robot is lightweight overall because of the use of light and integrated actuators. The robot can be applied as an agile mobile robot in the future. The robot also has multiple DoFs similar to those of humans, and it can thus perform as skillful shots as humans can. As an example, we demonstrated the spin net shot, which cannot be performed by previously developed badminton robots having a simple mechanism. A humanoid design also has excellent potential for entertainment or as a sparing partner taking advantage of its anthropomorphic design and motions.

As another contribution of this research, we expanded the possibilities of pneumatic robots. Pneumatic actuators are considered difficult to control owing to their slow response and high friction. A pneumatic robot is good at high-speed operation, but there have been few studies on robots that make use of the speed. In the present research, we conducted experiments on the accurate and high-speed operation of badminton motion performed by a pneumatic robot. The examination of reproducibility via a feedforward command showed that high reproducibility can be achieved even for high-speed swings. Using the result, we conducted an experiment in which the robot attempted to return a shuttle. The task required extremely high accuracy, yet the robot succeeded in returning the shuttle with high probability.

The robot proposed in this letter is a first step toward the development of a humanoid badminton robot, and can be extended to a humanoid arm or whole-body humanoid robot with more DoFs. In addition, our design will be applicable not only to the badminton robot but also to many kinds of robots that require high-speed motion, especially agile mobile robots having overall low weight; e.g., other sports robots and autonomous robots that quickly respond to unexpected events. However, we also discovered tasks to be tackled, such as those relating to sophistication of the whole system, countermeasures against deterioration, and the development of new training methods using simulation or machine learning. We suggested solutions but these topics are left for future work.

References

[1] H. Kitano, M. Asada, Y. Kuniyoshi, I. Noda, and E. Osawa, "RoboCup: The robot world cup initiative," in *Proc. ICAA*, 1997, pp. 340–347.

[2] K. Mülling, J. Kober, O. Kroemer, and J. Peters, "Learning to select and generalize striking movements in robot table tennis," *Int. J. Robot. Res.*, vol. 32, pp. 263–279, 2013.

[3] "ROBOCON 2015 - Indonesia," 2018. [Online]. Available: http://robocon.tvri.co.id/

[4] J. Stoev, S. Gillijns, A. Bartic, and W. Symens, "Badminton playing robot—A multidisciplinary test case in mechatronics," *IFAC Proc. Vol.*, vol. 43, pp. 725–731, 2010.

[5] T. Masunari *et al.*, "Shuttlecock detection system for fully-autonomous badminton robot with two high-speed video cameras," in *Proc. SPIE*, 2017, Art. no. 103281U.

[6] G. Waghmare, S. Borkar, V. Saley, H. Chinchore, and S. Wabale, "Badminton shuttlecock detection and prediction of trajectory using multiple 2 dimensional scanners," in *Proc. Int. Conf. Control, Meas. Instrum.*, 2016, pp. 234–238.

[7] *Guinness World Records 2015*. London, U.K.: Guinness World Records, 2015.

[8] A. Cooke, "Computer simulation of shuttlecock trajectories," *Sports Eng.*, vol. 5, pp. 93–105, 2002.

[9] C. M. Chan and J. S. Rossmann, "Badminton shuttlecock aerodynamics: Synthesizing experiment and theory," *Sports Eng.*, vol. 15, pp. 61–71, 2012.

[10] S. Kawamura, W. Choe, S. Tanaka, and S. R. Pandian, "Development of an ultrahigh speed robot FALCON using wire drive system," in *Proc. Int. Conf. Robot. Autom.*, 1995, vol. 1, pp. 215–220.

[11] T. Senoo, A. Namiki, and M. Ishikawa, "Ball control in high-speed batting motion using hybrid trajectory generator," in *Proc. Int. Conf. Robot. Autom.*, 2006, pp. 1762–1767.

[12] D. Büchler, H. Ott, and J. Peters, "A lightweight robotic arm with pneumatic muscles for robot learning," in *Proc. Int. Conf. Robot. Autom.*, 2016, pp. 4086–4092.

[13] "Barrett Technology, LLC—Products—WAM Arm," Barrett Technology, Newton, MA, USA, 2018. [Online]. Available: http://barrett.com/products-arm.htm

[14] A. S. Rambely, N. A. A. Osman, J. Usman, and W. A. B. W. Abas, "The contribution of upper limb joints in the development of racket velocity in the badminton smash," in *Proc. Int. Symp. Biomech. Sport*, 2005, pp. 422–426.

[15] K. Tanaka, S. Nishikawa, R. Niiyama, and Y. Kuniyoshi, "Humanoid robot performing jump-and-hit motions using structure-integrated pneumatic cable cylinders," in *Proc. Int. Conf. Humanoid Robot.*, 2017, pp. 696–702.

[16] K. Nakanishi, Learning Pneumatic Technology from the Basic in Japanese, Ohmsha, Ltd., Tokyo, Japan, 2001.

[17] D. Nguyen-Tuong and J. Peters, "Model learning for robot control: A survey," *Cogn. Process.*, vol. 12, pp. 319–340, 2011.